Table 3. Spectral and lag fit parameters using the model REFLAGS plus an extra Gaussian, and mixing the 2009 observation spectrum with the 2004 observation lags in the range 1–10 Hz.

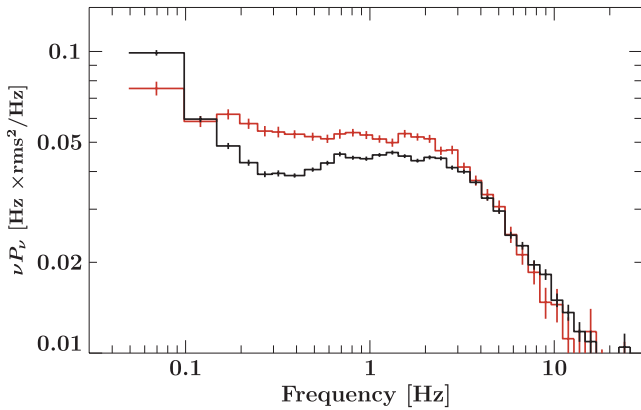| Parameter	Obs. A + extra line	Obs. B′
R_{in}/R_g	<60	<22
R_{out}/R_g	$(8.2^{+14.2}_{-3.6}) \times 10^3$	$(9.1^{+12.2}_{-3.5}) \times 10^3$
H_{out}/R_{out}	>0.06	<0.05
H_{src}/R_g	>80	>80
γ	>1.1	>1.0
i	<31.0	<30.2
Γ	1.459 ± 0.003	$1.4398^{+0.003}_{-0.009}$
$\log \xi$	<1.34	<1.31
E_c (keV)	6.85 ± 0.02	–
σ_c (keV)	0.25 ± 0.03	–
$\Omega^{eff}/(2\pi)$	0.81	0.86
χ^2 (spectrum)	1108	1449
χ^2 (time lags)	74	78
χ^2/dof	1182/1402	1527/1405

Figure 7. Power spectral densities for the 2004 (A, black) and 2009 (B, red) observations, in the energy range 2.0–10.0 keV.

range in frequency of the PSD (Fig. 7), where the PSD has a similar shape in both observations. Figs 8 and 9 show that when lags at frequencies <1 Hz are excluded, the model cannot successfully reproduce either the lag shape or amplitude.

4.1 Consistency of the reflection lags model with optical/UV data

The parameters inferred for the best-fitting reflection model, which are quite extreme and still do not provide a good fit to the lags, can also be checked for the implied effect on optical and UV emission from GX 339−4. X-ray heating of the outer disc could in principle produce a large optical/UV flux if there is a large solid angle illuminated by the continuum, as is the case for the geometry inferred from our lag model fits. We can assume that each illuminated cell in the disc absorbs a fraction of the illuminating continuum equal to $1 - a(E)$, so that the incident luminosity absorbed by each cell can be calculated for the best-fitting given continuum shape and model ionization parameter. If we make the simplifying assumption that the absorbed luminosity dominates over any intrinsic blackbody emission, we can equate the luminosity that is re-emitted by the cell to the absorbed luminosity and so determine the temperature of blackbody radiation emitted by each cell, and hence

determine the total reprocessed contribution to the spectral energy distribution (SED).

To compare the predicted contribution to the optical/UV SED from the geometry required by the lags model, we have extracted *Swift*/UVOT (bands *ubb*, *um*2, *uuu*, *uvv*, *uw*1, *uw*2, *uwh*) spectra from a 1760-s observation of GX 339−4 made on 29 March 2009, two days after *XMM–Newton* observed the source. uvot2pha was used to extract spectra for source and background using a 6-arcsec radius, as well as extract response files. No additional aspect correction was required.

From the best-fitting spectral parameters found in fit B′ and assuming a high-energy cut-off at 100 keV (Motta, Belloni & Homan 2011), we derive an X-ray luminosity of 3.5×10^{37} erg s^{-1} (assuming $d = 8$ kpc; Zdziarski et al. 2004). This value can be used to predict the reprocessed fluxes that are consistent with the geometries inferred from the fits, accounting for interstellar extinction using the XSPEC model REDDEN.

Fig. 10 shows the expected reprocessed spectra for the two fits to the 2009 X-ray data (orange for B, red for B′ and black is the 2009 X-ray spectrum). The photon index Γ of the power law that characterizes the reprocessed spectra at the energies covered by the UVOT data is −0.97. In these energy ranges, dust extinction needs to be taken into account using the multiplicative model REDDEN (Cardelli, Clayton & Mathis 1989). $E(B - V) = 0.933$ is the value for the extinction calculated from infrared dust maps along the line of sight towards our source.[1] By fitting a power law with a photon index of −0.97 to the UVOT data, one finds the unabsorbed intrinsic power law depicted in blue, which has a normalization in the UVOT energy range that is several decades larger than that expected from reprocessing, and requires $E(B - V) = 1.587$ for χ^2/dof = 0.8/4. Therefore, the model severely underpredicts the observed flux. A more likely explanation for the optical/UV emission is flat-spectrum synchrotron emission from a compact jet (Maitra et al. 2009) or magnetized hot accretion flow (Veledina, Poutanen & Vurm 2011). Assuming a power-law photon index of 1.0 (spectral energy index of 0), one also obtains a good fit (χ^2/dof = 0.64/4) and a lower extinction than in the previous case, $E(B - V) = 1.089$ (light blue line). This is consistent with the results found by Maitra et al. (2009) for the same object, fitting broad-band data using only synchrotron and inverse Compton models. Therefore, the UVOT data cannot be explained solely by reprocessing in the flared disc envisaged by the lags model and is more likely to be produced by a synchrotron process. However, a small contribution from reprocessing cannot be ruled out.

5 DISCUSSION

5.1 Physical implications

The analysis shown in Section 4 shows that extreme disc geometries are preferred for the model to reproduce the observed lags as closely as possible within the constraints given by the overall spectral shape, including the strength of the iron feature at 6.4 keV. There are several effects of the reprocessing geometry on the spectral and lag data that need to be highlighted to understand why the spectrum can be fitted well, whereas the lags cannot.

First, while the amount of flux in the iron line is proportional to the solid angle subtended by the disc, the ability to determine how much of it is produced in the outer radii of the disc (where Doppler
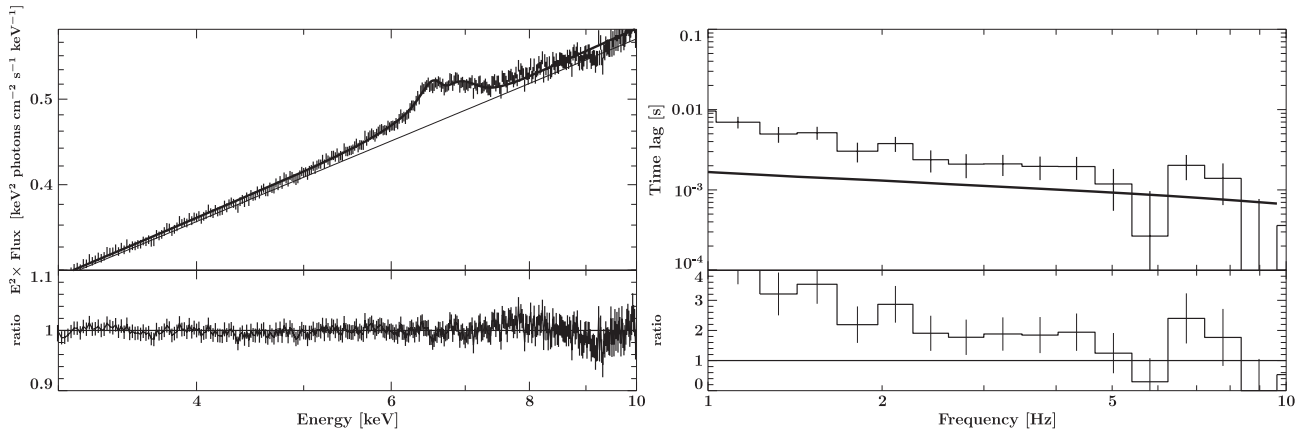
---

[1] http://irsa.ipac.caltech.edu/

Figure 8. Obs. A (2004 spectrum, left) and lags versus frequency (right). The thick solid lines represent the model REFLAGS (including a Gaussian component in the case of the spectrum) for the best-fitting parameters (see Table 3, column 2), in the frequency range 1–10 Hz.
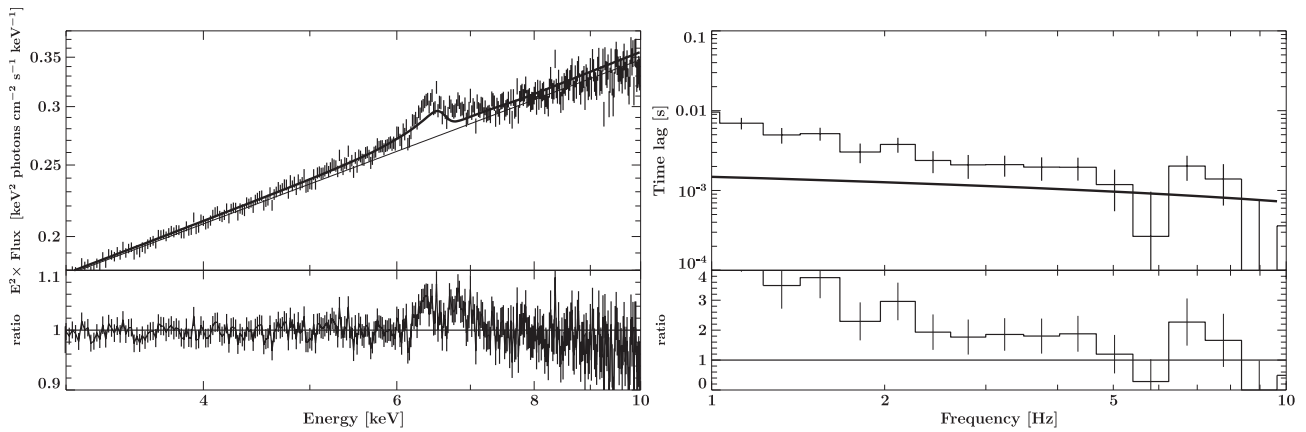

Figure 9. Obs. B′ (2009 spectrum, 2004 lags) spectrum (left) and lags versus frequency (right). The thick solid lines represent the model REFLAGS for the best-fitting parameters (see Table 3, column 3), in the frequency range 1–10 Hz.

effects are weak) is limited by the resolution of the *XMM–Newton* EPIC-pn detector. Therefore, the description of the geometry that could be inferred by the spectral modelling alone is degenerate, since line emission from the largest radii (e.g. $\sim 10^5 R_g$) cannot be resolved from that at more modest (but still large) radii (e.g. $\sim 10^4 R_g$). The result of this effect is that the spectral fits are not sensitive to variations in the outer radius of the reflector at large radii.

On the other hand, the lags are very sensitive to the geometry at large radii. First, the lags at low frequencies increase with both the solid angle and light-travel time to the reflector at large radii. A larger outer radius and more flared disc therefore corresponds to larger lags. However, the size-scale of the largest radius also corresponds to a characteristic low-frequency flattening in the lag versus frequency dependence. This is because the frequency-dependent drop in lags seen at higher frequencies is caused by smearing of the reflection variability on time-scales shorter than the light-travel size-scale of the reflector. The reflection variability amplitude is not smeared out for variability time-scales significantly longer than the light-travel time to the largest disc radii, and the lag at low frequencies quickly approaches the average light-travel delay from the reflector (diluted by the direct continuum emission which has zero intrinsic lag). The frequency of this characteristic flattening in the lag–frequency dependence is therefore a sensitive indicator of the size-scale of the reflector. However, it is not possible to reconcile

the position of this flattening at frequencies ~ 0.2 Hz with the large amplitude of the lags at low frequencies, which imply an even larger reflector subtending an even greater solid angle to the continuum at large radii.
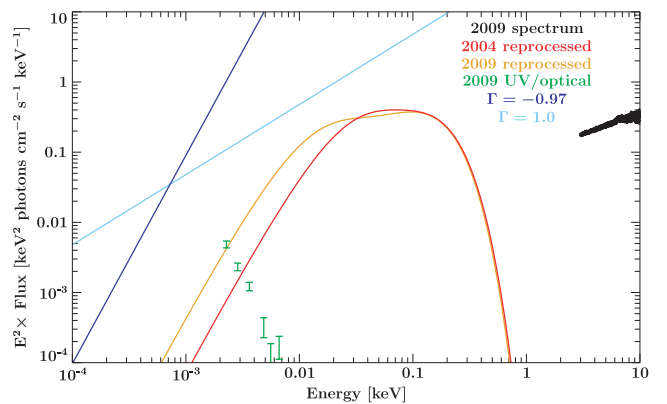

Figure 10. Comparison between expected reprocessed emission using the 2009 spectrum with 2004 lags (red) and 2009 lags (orange) and power-law fits to the data with photon indices −0.97 (same as the low energy tail of reprocessed spectra, in blue) and 1.0 (as expected from synchrotron emission coming from a jet, in light blue) after removing extinction. The data points from UVOT are shown in green.
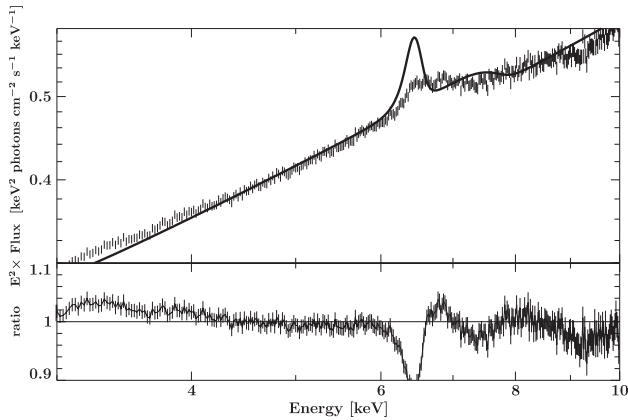
Figure 11. Spectral model (REFLAGS) compared to the 2004 spectrum using the parameters that are derived from fitting the 2004 lags alone. The lower panel shows the ratio data/model.

The result of these effects is that despite the already extreme inferred geometries the model is clearly underpredicting the lags. At this point, the maximum value of the lags is now constrained by the spectral modelling, which cannot place a tight constraint on the disc outer radius but does limit the solid angle of the reflector. It is instructive to consider the effects on the predicted spectral shape when the model is fitted to the 2004 lags alone (fixing $\Gamma = 1.5$) and the same parameters are used to estimate the resulting spectrum. This yields $\chi^2/\text{dof} = 66.4/16 = 4.15$ for the fit to the lags and yields an apparent solid angle $\Omega^{\text{eff}}/2\pi = 1.51$ subtended by the disc. The resulting spectral shape is compared to the data in Fig. 11. Therefore, even fitting the lag data alone with the model cannot produce a good fit, and the fit that is obtained shows that much larger solid angles of large-scale reflection are required than are permitted by the spectrum.

The lags cannot be explained solely by reflection; it is therefore necessary to invoke an additional mechanism to explain them. This result is perhaps not surprising, since we have previously found evidence that in hard state BHXRBs, fluctuations in the accretion disc blackbody emission are correlated with and precede the variations in power-law emission (Uttley et al. 2011). Although the disc variations seem to drive the power-law variations, this does not in itself explain the lags within the power-law band, which we consider in this paper, since the disc emission only extends up to ~2 keV. However, as we noted in Uttley et al. (2011), at frequencies <1 Hz, the lags of the power-law emission relative to the disc-dominated 0.5–0.9 keV band show a similar frequency dependence to the lags seen within the power-law band (i.e. $\tau \propto \nu^{-0.7}$). This strongly suggests that the lags intrinsic to the power law are somehow connected to the mechanism which causes the power law to lag the disc, most probably due to the propagation of accretion fluctuations through the disc before reaching the power-law emitting hot flow.

One possibility is that the disc is sandwiched by the hot-flow/corona which produces power-law emission which becomes harder towards smaller radii, leading to hard lags as fluctuations propagate inwards (e.g. Kotov et al. 2001; Arévalo & Uttley 2006). This model can explain the hard lags in terms of propagation times in the flow, which are much larger than light-crossing times and so can produce relatively large lags which the reflection model struggles to produce without leading to solid angles of large-scale reflection. Reflection may also contribute to the lags at some level, but is not the dominant mechanism, at least at frequencies <1 Hz.

© 2012 The Authors, MNRAS **422**, 2407–2416
Monthly Notices of the Royal Astronomical Society © 2012 RAS

A more detailed analysis of the contribution of reflection to the observed lags could be performed using data sets with higher signal-to-noise ratio, by e.g. searching for reflection signatures around the iron line investigated by Kotov et al. (2001). Lags versus energy spectra for GX 339−4 are shown in Uttley et al. (2011) for the 2004 *XMM–Newton* observation, and demonstrate that the current quality of the data is not sufficient to detect these features.

It is also possible that multiple distinct components contribute to the lag, e.g. associated with the different Lorentzian features that contribute to the PSD. This possibility could explain the apparent 'stepping' of the lag versus frequency that appears to be linked to the frequencies where the dominant contribution to the PSD changes from one Lorentzian component to another (Nowak 2000).

5.2 Wider implications of combined spectral-timing models

In this work we have considered (and ruled out) a relatively simple model for the lags in terms of the light-travel times from a large-scale reflector. However, it is important to stress the generalizability of our approach to other models. In particular, we have shown how it is possible to combine timing and spectral information to fit models for the geometry and spatial scale of the emitting regions of compact objects. Previous approaches to use the information from time lags to fit models for the emitting region have focused on fitting the lag data (e.g. Kotov et al. 2001; Poutanen 2002). However, since these models also make predictions for the spectral behaviour, it is possible to achieve stronger constraints on the models by fitting the lags together with the time-averaged energy spectrum, as done here, or with spectral-variability products such as the frequency-resolved rms and covariance spectra (Revnivtsev, Gilfanov & Churazov 1999; Wilkinson & Uttley 2009; Uttley et al. 2011).

In order to use these techniques more generally, one needs to calculate the energy-dependent response function for the emitting region, i.e. determine the emission as a function of time delay and energy. This approach can be used to test reverberation models for the small soft lags seen at high frequencies in active galactic nuclei (Fabian et al. 2009; Zoghbi et al. 2010; de Marco et al. 2011; Emmanoulopoulos et al. 2011) and BHXRBs (Uttley et al. 2011), which offers the potential to map the emitting region on scales within a few gravitational radii of the black hole. Other models can also be considered, e.g. to test the propagation models for the low-frequency lags with the time delay expressed in terms of propagation time through the accretion flow. Future, large-area X-ray detectors with high time and energy resolution, such as the proposed *ATHENA* and *LOFT* missions, will allow much more precise measurements of the lags in combination with good spectral measurements, so that fitting of combined models for spectral and timing data could become a default approach for studying the innermost regions of compact objects. Future research in this direction is strongly encouraged.

Infrared Science Archive, which is operated by the Jet Propulsion Laboratory, California Institute of Technology, under contract with the National Aeronautics and Space Administration.

REFERENCES

Arévalo P., Uttley P., 2006, MNRAS, 367, 801
Ballantyne D. R., Iwasawa K., Fabian A. C., 2001, MNRAS, 323, 506
Bendat J. S., Piersol A. G., 2010, Random Data: Analysis and Measurement Procedures. Wiley, New York
Cardelli J. A., Clayton G. C., Mathis J. S., 1989, IAU Symp., 135, 5
Cui W., Zhang S. N., Focke W., Swank J. H., 1997, ApJ, 484, 383
de Marco B., Ponti G., Uttley P., Cappi M., Dadina M., Fabian A. C., Miniutti G., 2011, MNRAS, 417, L98
Done C., Diaz Trigo M., 2010, MNRAS, 407, 2287
Emmanoulopoulos D., McHardy I. M., Papadakis I. E., 2011, MNRAS, 416, L94
Fabian A. C., Ross R. R., 2010, Space Sci. Rev., 157, 167
Fabian A. C., Rees M. J., Stella L., White N. E., 1989, MNRAS, 238, 729
Fabian A. C. et al., 2009, Nat, 459, 540
George I. M., Fabian A. C., 1991, MNRAS, 249, 352
Giannios D., 2005, A&A, 437, 1007
Kazanas D., Hua X.-M., Titarchuk L., 1997, ApJ, 480, 735
Kotov O., Churazov E., Gilfanov M., 2001, MNRAS, 327, 799
Kuster M., Kendziorra E., Benlloch S., Becker W., Lammers U., Vacanti G., Serpell E., 2002, preprint (arXiv:astro-ph/0203207)
Kylafis N. D., Papadakis I. E., Reig P., Giannios D., Pooley G. G., 2008, A&A, 489, 481
Lyubarskii Y. E., 1997, MNRAS, 292, 679

Maccarone T. J., Coppi P. S., Poutanen J., 2000, ApJ, 537, L107
Maitra D., Markoff S., Brocksopp C., Noble M., Nowak M., Wilms J., 2009, MNRAS, 398, 1638
Miyamoto S., Kitamoto S., Mitsuda K., Dotani T., 1988, Nat, 336, 450
Motta S., Belloni T., Homan J., 2009, MNRAS, 400, 1603
Nowak M. A., 2000, MNRAS, 318, 361
Nowak M. A., Vaughan B. A., Wilms J., Dove J. B., Begelman M. C., 1999, ApJ, 510, 874
Poutanen J., 2001, Adv. Space Res., 28, 267
Poutanen J., 2002, MNRAS, 332, 257
Poutanen J., Fabian A. C., 1999, MNRAS, 306, L31
Reig P., Kylafis N. D., Giannios D., 2003, A&A, 403, L15
Revnivtsev M., Gilfanov M., Churazov E., 1999, A&A, 347, L23
Tomsick J. A., Yamaoka K., Corbel S., Kaaret P., Kalemci E., Migliari S., 2009, ApJ, 707, L87
Uttley P., Wilkinson T., Cassatella P., Wilms J., Pottschmidt K., Hanke M., Böck M., 2011, MNRAS, 414, L60
Veledina A., Poutanen J., Vurm I., 2011, ApJ, 737, L17
Wilkinson T., 2011, PhD thesis, Univ. Southampton
Wilkinson T., Uttley P., 2009, MNRAS, 397, 666
Zdziarski A. A., Gierliński M., Mikołajewska J., Wardziński G., Smith D. M., Harmon B. A., Kitamoto S., 2004, MNRAS, 351, 791
Zoghbi A., Fabian A. C., Uttley P., Miniutti G., Gallo L. C., Reynolds C. S., Miller J. M., Ponti G., 2010, MNRAS, 401, 2419

This paper has been typeset from a TEX/LATEX file prepared by the author.